

DEFORMING HYPERBOLIC HEXAGONS WITH APPLICATIONS TO THE ARC AND THE THURSTON METRICS ON TEICHMÜLLER SPACES

ATHANASE PAPADOPOULOS AND SUMIO YAMADA

ABSTRACT. For each right-angled hexagon in the hyperbolic plane, we construct a one-parameter family of right-angled hexagons with a Lipschitz map between any two elements in this family, realizing the smallest Lipschitz constant in the homotopy class of this map relative to the boundary. As a consequence of this construction, we exhibit new geodesics for the arc metric on the Teichmüller space of an arbitrary surface of negative Euler characteristic with nonempty boundary. We also obtain new geodesics for Thurston's metric on Teichmüller spaces of hyperbolic surfaces without boundary. Our results generalize results obtained in the two papers [8] and [9].

AMS Mathematics Subject Classification: 32G15; 30F30; 30F60; 53A35.

Keywords: hyperbolic geometry; Teichmüller space; arc metric; geodesic; Lipschitz map; Thurston's metric; deforming hyperbolic hexagons.

1. INTRODUCTION

The Teichmüller space of a surface admits several natural metrics, starting with the Teichmüller metric introduced by Teichmüller in 1939, followed by the Weil-Petersson metric introduced by Weil in 1958, and there are many others. It is reasonable to say that the next metric which is most actively investigated today is the one introduced by Thurston in 1985 or 1986, which carries now the name Thurston's metric. These three metrics, along with others defined on Teichmüller space, were studied from various points of view: the infinitesimal structure (Finsler or Riemannian), the geodesics, the convexity properties, the isometries, the quasi-isometries, the curvature properties, the boundary structure, etc. Some basic questions concerning these properties were solved and others, more difficult, remain open and make the subject a living one.

In the present paper, the setting is the non-reduced Teichmüller theory of surfaces with boundary. We mean by this that the homotopies that we consider, in the definition of the equivalence relation defining Teichmüller space, do not necessarily fix pointwise the boundary of the surface. In general, the metrics on Teichmüller space were defined for closed surfaces or surfaces with punctures (or distinguished points). Some of these metrics, like the Teichmüller metric, admit a straightforward generalization to the case of surfaces with boundary, but other metrics do not generalize as such, and one has to modify their definition to make them fit to surfaces with boundary. One example is Thurston's metric, whose modification, the so-called arc metric, was studied in the papers [2], [6], [8], [9]. We shall recall the definition of the arc metric below. Several basic questions concerning this metric still resist. For instance, it is unknown whether it is Finsler, its isometry

Date: January 25, 2017.

Athanase Papadopoulos was partially supported by the grant ANR-12-BS01-0009 (Géométrie de Finsler et applications).

Sumio Yamada was partially supported by JSPS KAKENHI 24340009 and 16K13758.

group is still not identified, and it is unknown whether this metric coincides with the Lipschitz metric. (All these results are known for Thurston's metric.) In the present paper, we construct new families of geodesics for this metric. In order to state more precisely the results, we start with some notation.

Let S be a surface of finite type with nonempty boundary. The hyperbolic structures on S that we consider are such that the boundary components are closed geodesics.

A simple closed curve on S is *essential* if it is neither homotopic to a point nor to a puncture (but it can be homotopic to a boundary component).

An *arc* on S is the image of a compact interval of \mathbb{R} by a proper embedding, that is, the interior of the arc is embedded in the interior of S and its endpoints are on the boundary of S . In this paper, when we deal with homotopies of arcs, we only consider homotopies that are relative to ∂S , that is, they keep the endpoints of the arc on the boundary of the surface (but they do not necessarily fix pointwise the points of that boundary). An arc is *essential* if it is not homotopic to an arc contained in ∂S .

We shall use the following notation:

\mathcal{B} is the union of the set of homotopy classes of essential arcs on S and the set of homotopy classes of simple closed curves homotopic to a boundary component of S .

\mathcal{S} is the set of homotopy classes of essential simple closed curves on S .

Suppose that the surface S is equipped with a hyperbolic structure g . In any homotopy class of essential arc in S , there is a unique geodesic arc whose length is minimal among the arcs in that class relative the boundary. This geodesic arc makes at its endpoints right angles with the boundary of S . We denote by $\ell_\gamma(g)$ the length of this geodesic arc, and we call it the *geodesic length* of γ for the hyperbolic metric g . Likewise, for any element γ of \mathcal{S} , we denote by $\ell_\gamma(g)$ the length of its unique geodesic representative for the hyperbolic metric g .

Let $\mathcal{T}(S)$ be the Teichmüller space of S . We view $\mathcal{T}(S)$ as the space of homotopy classes of hyperbolic structures on S with geodesic boundary, where the lengths of the boundary components are not fixed. The *arc metric* \mathcal{A} on $\mathcal{T}(S)$ is defined by the formula

$$(1) \quad \mathcal{A}(g, h) = \sup_{\gamma \in \mathcal{B} \cup \mathcal{S}} \log \frac{\ell_\gamma(h)}{\ell_\gamma(g)}$$

where g and h are hyperbolic structures on S . This is an asymmetric metric (that is, it satisfies all the axioms of a metric except the symmetry axiom). It was introduced in [5] and it is an analogue for surfaces with boundary of Thurston's asymmetric metric on the Teichmüller space of a surface without boundary (possibly with cusps) [10]. It was shown in [5] (Proposition 2.13) that one obtains the same metric by using Formula (1) except that the supremum is taken now over \mathcal{B} instead of $\mathcal{B} \cup \mathcal{S}$. In other words, we also have

$$(2) \quad \mathcal{A}(g, h) = \sup_{\gamma \in \mathcal{B}} \log \frac{\ell_\gamma(h)}{\ell_\gamma(g)}$$

The arc metric is studied in the papers [2], [6], [8] and [9].

We now recall the definition of the Lipschitz metric on the Teichmüller space of a surface with boundary. The definition is the same as the one of the Lipschitz metric defined by Thurston on Teichmüller spaces of surfaces without boundary.

One first defines the *Lipschitz constant* of a homeomorphism $f : (X, d_X) \rightarrow (Y, d_Y)$ between two metric spaces by the formula

$$(3) \quad \text{Lip}(f) = \sup_{x \neq y \in X} \frac{d_Y(f(x), f(y))}{d_X(x, y)} \in \mathbb{R} \cup \{\infty\}.$$

The homeomorphism f is said to be *Lipschitz* if its Lipschitz constant is finite.

Given an ordered pair of hyperbolic structures g and h on S , the *Lipschitz distance* between them (and between the corresponding points in the Teichmüller space $\mathcal{T}(S)$) is defined as

$$(4) \quad L(g, h) = \log \inf_{f \sim \text{Id}_S} \text{Lip}(f)$$

where the infimum is taken over all homeomorphisms $f : (S, g) \rightarrow (S, h)$ in the homotopy class of the identity of S .

In the case of surfaces without boundary, Thurston's metric and the Lipschitz metric coincide. This is a result of Thurston in [10]. It is unknown whether in the case of surfaces with boundary the Lipschitz and the arc metrics coincide.

In Thurston's theory for surfaces without boundary developed in [10], maps between ideal triangles are the building blocks for the construction of geodesics for Thurston's metric on Teichmüller space. The geodesics obtained in this way are the so-called "stretch lines" and Thurston proves that any two points in the Teichmüller space of S are joined by a concatenation of finitely many stretch lines. It is possible to construct a class of geodesics for the arc metric \mathcal{A} using Thurston's method for stretch lines. For this, a complete maximal geodesic lamination is needed (in the language of [10], this will be the geodesic lamination which is maximally stretched); for instance, we can take a lamination whose leaves spiral along the boundary components of the surface S . We then apply Thurston's method described in [10] for the construction of stretch lines using the stretch maps between ideal triangles and gluing them over all the ideal triangles that are the connected components of the complement of the lamination. To see that the one-parameter family of surfaces obtained in this way is a geodesic for the arc metric \mathcal{A} , one can double the surface S along its boundary components and consider the resulting one-parameter family of hyperbolic structures on the doubled surface S^d . This is a geodesic for Thurston's metric on S^d . The restriction to S of this one-parameter family of deformations of hyperbolic structures is a geodesic for the metrics \mathcal{A} and L on the Teichmüller space of the surface with boundary. A geodesic for the arc metric defined in this way is of a special type (that is, not all geodesics for the arc metric are obtained in this manner). Along this geodesic, the lengths of all the geodesic boundary components of S are multiplied by the same constant factor.

Another construction of \mathcal{A} -geodesics in the setting of surfaces with boundary is obtained by taking as building blocks right-angled hexagons instead of ideal triangles. In the present paper, we shall introduce canonical maps between such hexagons which depend on a parameter K . By varying K we obtain geodesics for the arc metric. Each right-angled hexagon belongs to such a family of deformations, and between each pair of hexagons of the same family we exhibit a Lipschitz map that realizes the best Lipschitz constant in its homotopy class relative to the boundary. Gluing the hexagons along pieces of their boundaries, we obtain deformations of the hyperbolic surfaces that are geodesics for the arc metric. These geodesics are also geodesic for the Lipschitz metric and the arc and the Lipschitz metrics coincide on these lines. By gluing surfaces with boundary along their boundary components, we obtain geodesics for Thurston's metric that are different from the stretch lines. This generalizes the set of results obtained in the two papers [8] and [9].

2. GEOMETRY OF RIGHT-ANGLED HEXAGONS

2.1. Three types of right-angled hexagons. For the construction of Lipschitz maps between arbitrary right-angled hexagons, we shall divide such a hexagon H into three regions (one such region may possibly be empty) which carry natural coordinates; that is, the points in such a region are parametrized by pairs of real numbers. The coordinates in each region are induced by a pair of orthogonal foliations F and G on H , which we now define.

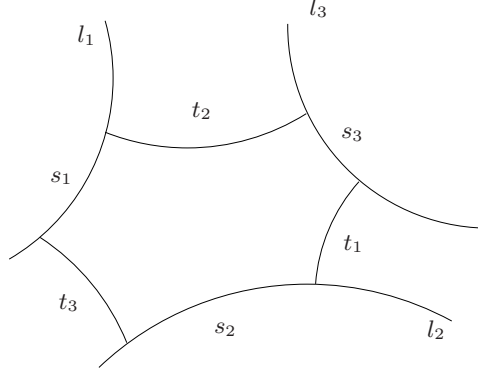


FIGURE 1. Six geodesic lines enclosing a hexagon.

We consider three pairwise non-consecutive edges t_1, t_2, t_3 of a right-angled hexagon H , and we call them the *short edges*. The three lengths $\lambda_1, \lambda_2, \lambda_3$ of t_1, t_2, t_3 may or may not satisfy the triangle inequality. Up to a permutation of the indices, there are three cases:

- (1) Type I: $\lambda_1, \lambda_2, \lambda_3$ satisfy the three strict triangle inequalities.
- (2) Type II: $\lambda_1 + \lambda_2 = \lambda_3$.
- (3) Type III: $\lambda_1 + \lambda_2 < \lambda_3$.

We now give another characterization of the three distinct types.

Recall that two geodesic lines in the hyperbolic plane are said to be hyper-parallel when they intersect each other neither in the hyperbolic plane, nor on the geometric boundary of this plane. In the case where the geodesics intersect each other on the boundary, the geodesics are said to be *asymptotic*, or *parallel*.

Consider three pairwise hyper-parallel geodesic lines l_1, l_2, l_3 in the hyperbolic plane, relatively positioned so that for each geodesic l_i , the other two geodesics l_j, l_k , ($j, k \neq i$) lie on the same side of l_i . In particular, we are excluding the possibility that some l_i and l_j are asymptotic to each other. Each pair l_i, l_j ($i \neq j$) has a common perpendicular geodesic segment t_k ($k \neq i, j$). This common perpendicular segment, which we call a *short edge*, is unique. We denote by $\tilde{l}_1, \tilde{l}_2, \tilde{l}_3$, the three geodesic lines that contain the short edges t_1, t_2, t_3 respectively. The six geodesic lines $l_1, l_2, l_3, \tilde{l}_1, \tilde{l}_2, \tilde{l}_3$ enclose a hexagon with six right angles (Figure 1). The side opposite to a short edge t_i will be denoted by $s_i \subset l_i$, and called a *long edge*.

There exists a unique point O which is equidistant from $\tilde{l}_1, \tilde{l}_2, \tilde{l}_3$. The three types listed above correspond respectively to the cases where the point O lies inside the right-angled hexagon H (Type I), or on one of the long edges s_i (Type II), or outside H (Type III); cf. Figure 2.

One should be aware of the fact that interchanging the short and long edges of a given right-angled hexagon makes the resulting center O different from the original center unless the hexagon has a \mathbb{Z}_3 -rotational symmetry.

From now on, when we refer to a right-angled hexagon, it will be understood that a choice of short and long edges has been made.

2.2. The tripod and the hypercycle foliation of a right-angled hexagon.

A right-angled hexagon H is naturally equipped with a measured foliation which is a union of three foliated regions F_1, F_2, F_3 with disjoint interiors (one of them may be empty). We explain below the construction of this foliation.

For each $i = 1, 2, 3$, we consider the orthogonal projection of O onto the geodesic $\tilde{l}_i \supset t_i$, which we denote by A_i . We obtain a tripod T whose edges OA_1, OA_2 and OA_3 have equal lengths $d > 0$, and where each edge OA_i meets \tilde{l}_i perpendicularly. In Figure 2, we have represented the tripod in the three cases of hexagons (Types I, II and III).

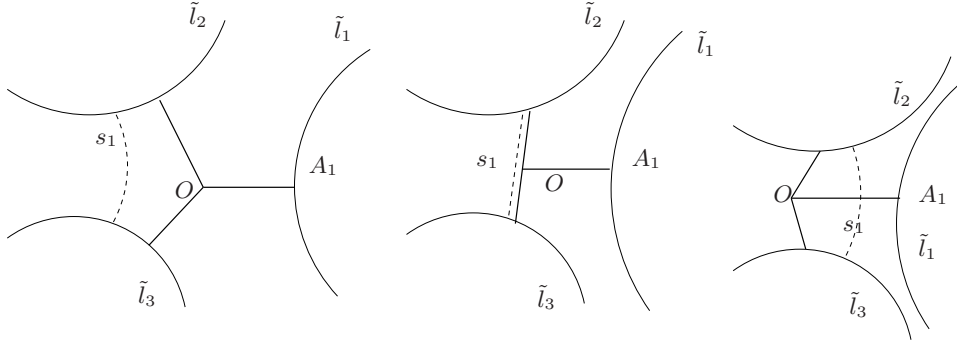


FIGURE 2. The tripod is drawn in bold lines. The center O of the hexagon may be in the interior of the hexagon (figure to the left, Type I), or on one side (the side s_1 in the figure in the middle, Type II), or outside the hexagon (figure to the right, Type III). In the case in the middle, the side s_1 (dashed line) coincides with the union of two edges of the tripod.

Choose one pair among the three tripod edges, say, OA_1 and OA_2 . The pair OA_1 and OA_2 and the long edge s_3 together with (part of) the short edges t_1 and t_2 bounds a region, which is a pentagon P_3 with four right-angled corners (Figure 3).

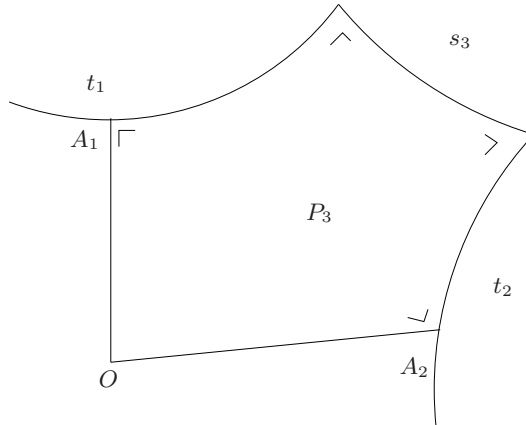


FIGURE 3. The pentagon P_3

Draw in P_3 a family of hypercycles each of which is a locus of equidistant points measured from the long edge s_3 . In the hyperbolic plane, equidistant points to

geodesics are classically called hypercycles, and we shall use this terminology. P_1 and P_2 are similarly defined.

For each $i = 1, 2, 3$, P_i consists of two regions R_i and C_i , where the former is foliated by hypercycles whose endpoints are on the long edge t_j and t_k for $j, k \neq i$, and the latter is foliated by hypercycles whose endpoints are on the tripod edges OA_j and OA_k . The foliation of P_i equipped with its foliation F_i is represented in Figure 4.

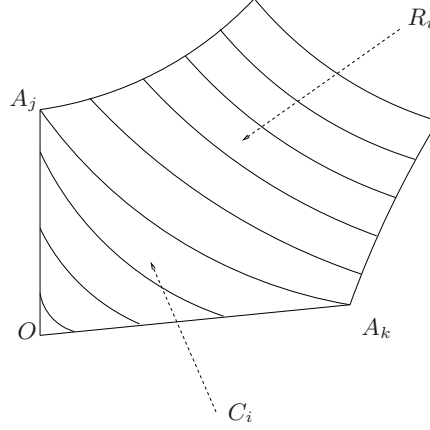


FIGURE 4. The pentagon P_i equipped with its foliation F_i .

We consider the region

$$\tilde{H} := P_1 \cup P_2 \cup P_3$$

For hexagons of Type I and II, \tilde{H} coincides with the right-angled hexagon H , and for Type III, \tilde{H} strictly contains H . The leaves of the three foliations F_1, F_2, F_3 may possibly intersect in \tilde{H} . Restrict the three foliations F_1, F_2, F_3 to the original hexagon H to obtain a foliation of H .

We call the union of three regions $(\cup_i C_i) \cap H$ the *central region* C of H .

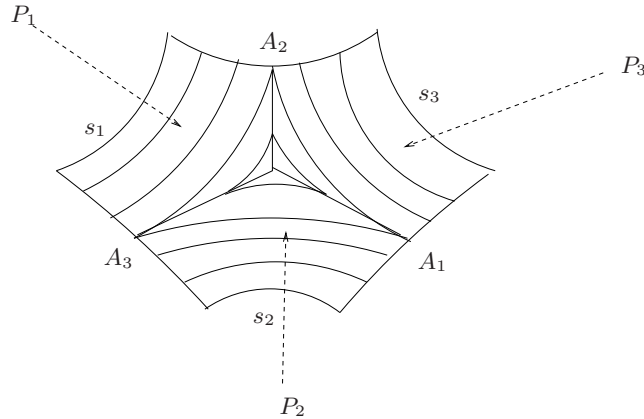


FIGURE 5. The hexagon H is the union of the three pentagons P_1, P_2, P_3 .

The supports of the foliations F_i by hypercycles restricted to $R_i \subset P_i$ have a natural structure of rectangles and these foliations are equipped with transverse measures induced from the Lebesgue measure on the boundaries of the supports,

whose total masses L_1, L_2, L_3 satisfy the equations

$$\begin{cases} \lambda_1 = L_2 + L_3 \\ \lambda_2 = L_1 + L_3 \\ \lambda_3 = L_1 + L_2. \end{cases}$$

with an appropriate meaning when one of the lengths L_i is negative, as we discuss now. This is represented in Figure 7 below.

For Type I, the central region C is bounded by the three hypercycles distant from s_i by $L_i > 0$ for each i and $C = C_1 \cup C_2 \cup C_3$. Types II and III correspond respectively to the cases when one of the total masses L_i , say L_3 , is zero or strictly negative, and the central region is bounded by two hypercycles and one boundary geodesic segment s_3 . In Types II and III, when $L_3 \leq 0$ (or equivalently when the set $\text{interior}(F_3) \cap H$ is empty) the strict triangle inequality

$$\lambda_1 + \lambda_2 > \lambda_3$$

among the lengths of the short sides is not satisfied. The three types of foliations corresponding to Types I, II and III are represented in Figure 6.

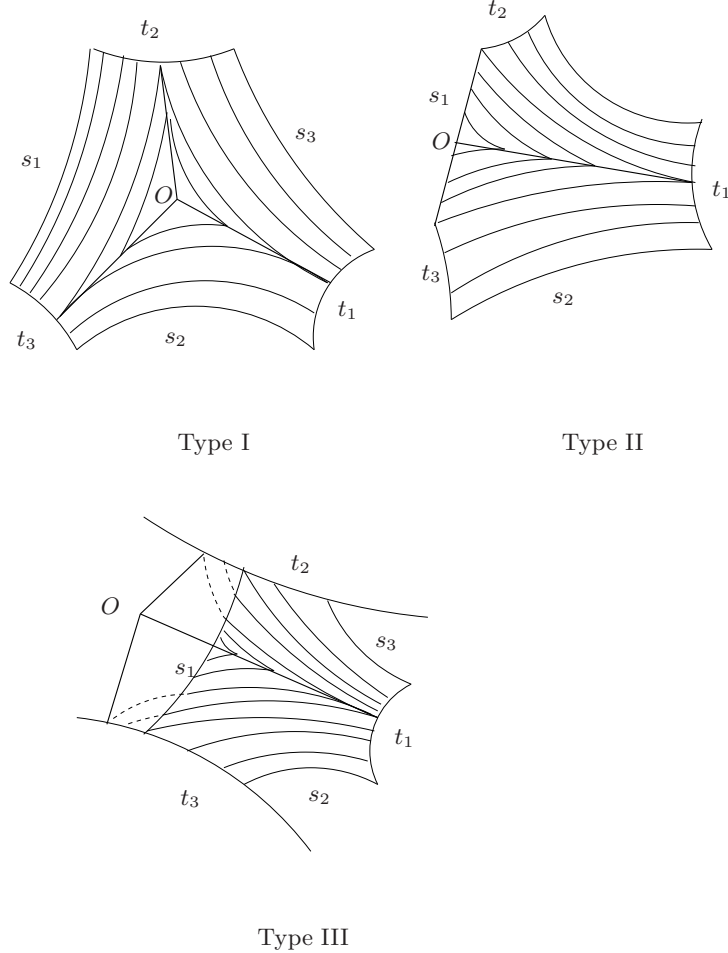


FIGURE 6. The three types of hypercycle foliations of a right-angled hexagon.

In Type I, corresponding to the case to the left picture of Figures 2 and 6, for each $i = 1, 2, 3$, A_i divides each short edge t_i at an inner point. In this case L_1, L_2, L_3

are all positive. In Type II, two of the points A_i , say A_2 and A_3 , coincide with endpoints of t_2 and t_3 respectively. In this case, we have $L_1 = 0$ and the foliation H is of the type depicted on the upper right hexagon of Figure 6. Finally, Type III corresponds to the case where two of the A_i , say A_2 and A_3 , divide the short edges t_2 and t_3 externally. In this case we have $L_1 < 0$, and the foliation H is as depicted in the bottom hexagon of Figure 6, and in Figure 7.

We now look into the Type I case more closely using the Poincaré disc model and taking the point O at the center of this disc. The hexagon H is divided into three

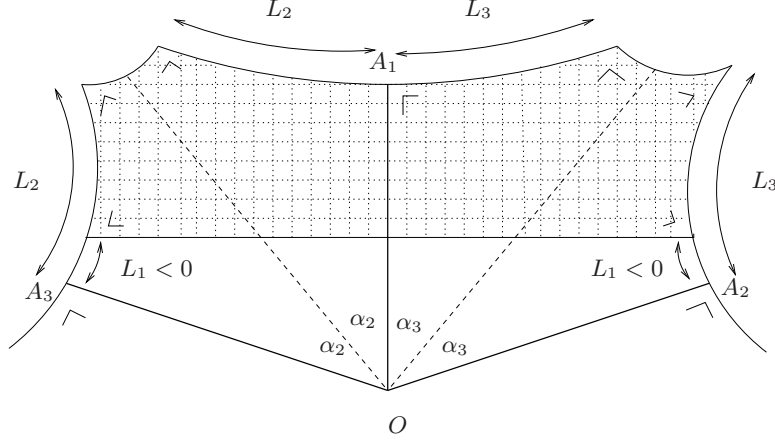


FIGURE 7. The shaded region represents a Type III hexagon. The tripod is represented in bold lines. The point O lies outside H .

pentagons P_1, P_2, P_3 by the geodesic tripod $T = \cup_{i=1}^3 \overline{OA_i}$ whose edges have the same hyperbolic length d , each edge meeting one of the short edges perpendicularly. Each pentagon P_i is foliated by pieces of hypercycles which are equidistant from the long edges s_i of H , and the hexagon H is foliated as a union of three foliations F_i ($i = 1, 2, 3$) (Figure 5). The pentagon P_i has a \mathbb{Z}_2 -symmetry across the angle bisector of $\angle A_j O A_k$ ($j, k \neq i$).

For each $i = 1, 2, 3$, the value of the angle between OA_j and OA_k ($j, k \neq i$) is set to be equal to $2\alpha_i$. (The half-values, α_i , will play a role below.)

The Type II hexagon is a limiting case of the Type I hexagon, where the two edges $\overline{OA_2}$ and $\overline{OA_3}$ form an angle $2\alpha_1 = \pi$. In this case, two edges of the tripod are aligned, the pentagon P_1 is collapsed to the long edge s_1 , and the hexagon is covered by the remaining two foliated regions. In other words, H is a union of two pentagons P_2 and P_3 whose central vertex angles at O satisfy $2\alpha_2 + 2\alpha_3 = \pi$.

In the Type III hexagon, represented in Figure 7, the region H is a proper subset of two pentagons P_2 and P_3 (these are the left and right halves of the hexagon pictured) with its central angles satisfying $2\alpha_2 + 2\alpha_3 < \pi$, or equivalently $2\alpha_1 > \pi$.

In what follows, we shall concentrate the discussion on Type I hexagons. Type II and III hexagons will be considered when needed.

2.3. Orthogonal coordinate system on right-angled hexagons. We equip each pentagon P_i with a second foliation G_i transverse to F_i whose leaves are the fibers of the nearest point projection map $\pi_i : P_i \rightarrow s_i$. It turns out that the leaves of this foliation are geodesics which intersect orthogonally the leaves of F .

In a Type I hexagon, we parameterize the leaves of the foliation F_i by $0 \leq u_i \leq 2$ as follows.

For each i , the region P_i is foliated by leaves $\{F_i(u_i)\}$ where $F_i(0)$ is the long edge s_i , $F_i(1)$ is the side of the central region in P_i , and $F_i(2)$ is the origin O (a degenerate

leaf). In between, for $0 < u_i < 1$, we interpolate the leaves proportionally to the hyperbolic distance from the long edge s_i . For $1 < u_i < 2$, the interpolation is done proportionally to the hyperbolic length along the edges of the geodesic tripod T .

We parametrize the leaves of G_i by $0 \leq v_i \leq 2$ such that $G_i(0)$ and $G_i(2)$ are parts of the short edges t_j, t_k with $j, k \neq i$ of length L_i sandwiching the long edge s_i , and such that $G_i(1)$ is the geodesic segment from the origin O meeting the long edge s_i perpendicularly at its midpoint and bisecting the central angle $2\alpha_i$ at O . This geodesic segment is shared by the two congruent quadrilaterals Q_i and \hat{Q}_i with $P_i = Q_i \cup \hat{Q}_i$. In between, the interpolation is done proportionally to hyperbolic length along the long edge s_i .

With this pair of foliations $\{(F_i, G_i)\}_{i=1,2,3}$ where the leaves are parameterized by u_i and v_i , the hexagon P_i has a coordinate system. Namely each point $p \in P_i \subset H$ is identified with an ordered pair (u_i, v_i) . Note that along the gluing edges of the three pentagons P_1, P_2 and P_3 , the parameters u_i and u_j with $i \neq j$ are compatible, that is, $u_i(p) = u_j(p)$ if p lies on the edge of the tripod between P_i and P_j .

A Type II and III hexagon H has a similar coordinate system, which is just the restriction of the three pentagons P_i to the hexagon H .

3. GEOMETRY OF HYPERBOLIC QUADRILATERALS WITH THREE RIGHT ANGLES

A congruent pair of hyperbolic geodesic quadrilaterals with three right angles with opposite orientations form a geodesic pentagon with four right angles (see Figure 10 below). We study in this section hyperbolic quadrilaterals with three right angles. We recall a set of classical formulae (see e.g. [4]) for such quadrilaterals, relating the side lengths and the non-right angle $\alpha < \pi/2$ of the quadrilateral. Such a quadrilateral is usually called a trirectangular quadrilateral.

We represent the quadrilateral in the Poincaré disc model of the hyperbolic plane. We assume that α is positioned at the origin O , with two edges being radial segments, one of which (the side OA) having length d and the other one (the side OC) having length $L + h$, where L is the length of the edge AB opposite to the side OC (see Figure 8). Finally, we denote the length of the side BC by ℓ . This quadrilateral is uniquely determined by the two values α and d . The trigonometric formulae are the following:

$$(5) \quad \frac{\cosh \ell}{\sin \alpha} = \frac{\cosh d}{\sin \frac{\pi}{2}} = \frac{\sinh(L + h)}{\sinh L}$$

$$(6) \quad \sinh \ell = \sinh d \cosh(L + h) - \cosh d \sinh(L + h) \cos \alpha$$

$$(7) \quad \sinh d = \sinh \ell \cosh(L + h) - \cosh \ell \sinh(L + h) \cos \frac{\pi}{2}$$

$$(8) \quad \cos \alpha = \sin \frac{\pi}{2} \sinh L \sinh \ell - \cos \frac{\pi}{2} \cosh L$$

$$(9) \quad \cos \frac{\pi}{2} = \sin \alpha \sinh L \sinh d - \cos \alpha \cosh L$$

$$(10) \quad \cosh(L + h) = -\sinh \ell \sinh d + \cosh \ell \cosh d \cosh L$$

$$(11) \quad \cosh L = \sin \alpha \cosh(L + h)$$

In these formulae, the angle $\pi/2$ is the right angle at the vertex C . In the book [4], the above formulae are given for a quadrilateral with two consecutive right angles, with the angle C not necessarily $\pi/2$. We have rewritten them in the special case $C = \pi/2$.

Now suppose that the value of the acute angle is $\pi - \alpha$ with $\alpha > \pi/2$. The set of formulae then becomes

$$\begin{aligned}
\frac{\cosh \ell}{\sin(\pi - \alpha)} &= \frac{\cosh d}{\sin \frac{\pi}{2}} = \frac{\sinh(L + h)}{\sinh L} \\
\sinh \ell &= \sinh d \cosh(L + h) - \cosh d \sinh(L + h) \cos(\pi - \alpha) \\
\sinh d &= \sinh \ell \cosh(L + h) - \cosh \ell \sinh(L + h) \cos \frac{\pi}{2} \\
\cos(\pi - \alpha) &= \sin \frac{\pi}{2} \sinh L \sinh \ell - \cos \frac{\pi}{2} \cosh L \\
\cos \frac{\pi}{2} &= \sin(\pi - \alpha) \sinh L \sinh d - \cos(\pi - \alpha) \cosh L \\
\cosh(L + h) &= -\sinh \ell \sinh d + \cosh \ell \cosh d \cosh L \\
\cosh L &= \sin(\pi - \alpha) \cosh(L + h).
\end{aligned}$$

By noting that $\cos(\pi - \alpha) = -\cos \alpha$, $\sin(\pi - \alpha) = \sin \alpha$, $\cosh(-x) = \cosh x$ and $\sinh(-x) = -\sinh x$, we can rewrite these formulae as

$$\begin{aligned}
(12) \quad \frac{\cosh \ell}{\sin \alpha} &= \frac{\cosh d}{\sin \frac{\pi}{2}} = \frac{\sinh[-(L + h)]}{\sinh(-L)} \\
(13) \quad \sinh \ell &= \sinh d \cosh[-(L + h)] - \cosh d \sinh[-(L + h)] \cos \alpha \\
(14) \quad \sinh d &= \sinh \ell \cosh[-(L + h)] - \cosh \ell \sinh[-(L + h)] \cos \frac{\pi}{2} \\
(15) \quad \cos \alpha &= \sin \frac{\pi}{2} \sinh(-L) \sinh \ell - \cos \frac{\pi}{2} \cosh(-L) \\
(16) \quad \cos \frac{\pi}{2} &= \sin \alpha \sinh(-L) \sinh d - \cos \alpha \cosh(-L) \\
(17) \quad \cosh[-(L + h)] &= -\sinh \ell \sinh d + \cosh \ell \cosh d \cosh(-L) \\
(18) \quad \cosh(-L) &= \sin \alpha \cosh[-(L + h)].
\end{aligned}$$

Formally, in comparing them with equations (5, 6, 7, 8, 9, 10, 11), these formulae describe the shape of a quadrilateral with three right angles and one obtuse angle $\alpha > \pi/2$, and negative lengths $-L$ and $-h$, even though there is no such hyperbolic quadrilateral since the non-right-angle of a trirectangular quadrilateral in the hyperbolic plane is always acute, and there are no *negative* side lengths. These algebraic expressions, however, can be interpreted as follows.

Since the isometry type of a trirectangular quadrilateral is uniquely determined (up to orientation) by $0 < \alpha < \pi/2$ and the side length $d > 0$, consider for a fixed d

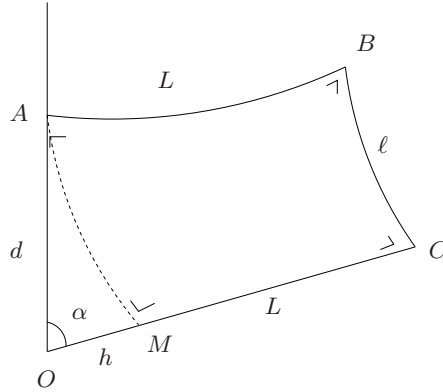


FIGURE 8. The dashed line AM is a piece of hypercycle parallel to the side BC . All the other lines are geodesics.

the family of quadrilaterals obtained by increasing α . When α approaches $\pi/2$, the side BC of length ℓ converges to the side OA , and the sides AB and OC collapse to the points A and O respectively. Thus, the quadrilateral becomes degenerate and we have $\ell = d$ and $L = h = 0$ in Equations (5), (6) and (7).

For $\alpha > \pi/2$ with the same $d > 0$, we identify the situation given by Equations (12, 13, 14, 15, 16, 17, 18) with a quadrilateral with vertex angle $\pi - \alpha$ appearing on the other side of OA , the image of the corresponding quadrilateral with the angle $\alpha - \pi/2$ across the side OA . The negative lengths $-L$ and $-h$ refer to the reflective symmetry across the side OA . The situation is represented in Figure 9.

In this sense, the set of equations (5, 6, 7, 8, 9, 10, 11) describes the moduli of quadrilaterals with a fixed $d > 0$ and variable vertex angle α , where α varies in $[0, \pi]$, where the corresponding quadrilaterals are possibly degenerate, and with the opposite orientations with respect to the symmetry across the side OA .

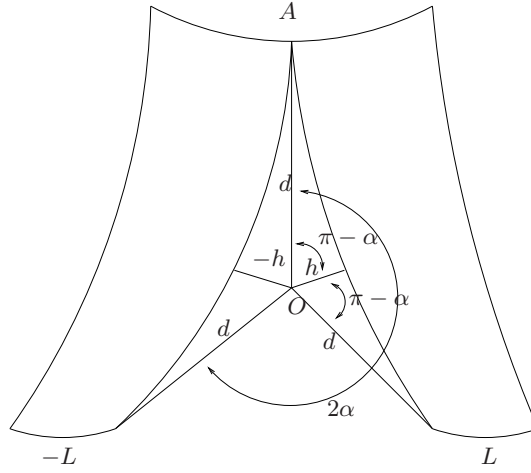


FIGURE 9. The trigonometric formulae (12)–(18) refer to the four right-angled pentagon on the left hand side. In this pentagon, the value of the angle at O is $2(\pi - \alpha)$, corresponding to the value 2α for the exterior angle.

4. ON THE GEOMETRY OF HEXAGONS MODELED ON THE POINCARÉ DISC

For a given trirectangular quadrilateral $Q = OABC$ with three right angles at the vertices A, B, C and one acute angle α at O , we consider the trirectangular quadrilateral \hat{Q} which is the mirror image of Q by the reflection through the straight edge OC . We denote the corresponding vertices of \hat{Q} by $\hat{A}, \hat{B}, \hat{O} = O$ and $\hat{C} = C$. The union of Q and \hat{Q} is a pentagon $P = OAB\hat{B}\hat{A}$ (Figure 10), where all the interior angles are right, except at the vertex O whose interior angle is 2α .

Now consider the situation where there are three pentagons P_1, P_2 and P_3 satisfying the compatibility condition $\alpha_1 + \alpha_2 + \alpha_3 = \pi$ with $\alpha_i < \pi/2$ for each i , and $d_1 = d_2 = d_3$, a common value which we denote by d . The three pentagons can be glued together via the identifications of the edges emanating from the origin O ,

$$\begin{aligned} OA_1 &\simeq O\hat{A}_2 \\ OA_2 &\simeq O\hat{A}_3 \\ OA_3 &\simeq O\hat{A}_1 \end{aligned}$$

to produce a right-angled hexagon H . This is the Type I case described before, and it is depicted in Figure 11.

The condition $\alpha_i < \pi/2$ is violated when $\alpha_1 = \pi/2$ and thus $\alpha_2 + \alpha_3 = \pi/2$. This is the case when P_1 degenerates to the line segment $A_2O \cup OA_3$, and the hexagon is just $P_2 \cup P_3$.

Finally when $\alpha_1 > \pi/2$, then $\pi - \alpha_1 < \pi/2$, and as described in the previous section, the quadrilateral Q_1 with its vertex angle $\pi - \alpha$ appears on the other side of OA_2 and \hat{Q}_1 on the other side of OA_3 . Consequently the pentagon $P_1 = Q_1 \cup \hat{Q}_1$ overlaps with P_2 and P_3 . This is the type III picture. Note that the compatibility condition among $\alpha_1, \alpha_2, \alpha_3$ is still intact since the vertex angle of P_1 at O is the sum of those of P_2 and P_3 :

$$\pi - \alpha_1 = \alpha_2 + \alpha_3.$$

Also note that by using the original $\alpha_1 > \pi/2$ in the set of equations (5, 6, 7, 8, 9, 10, 11), the resulting negativity of L_1 can now be understood with the observation we made in the case of Type III, in which the triangle inequality among λ_1, λ_2 and λ_3 is violated.

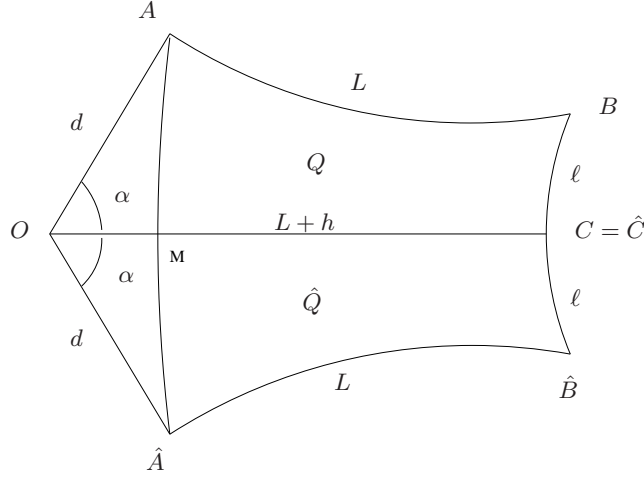


FIGURE 10. The pentagon is a union of two trirectangular quadrilaterals Q and \hat{Q} . In this figure, the lines AM and $\hat{A}M$ are hypercycles. All the other lines are geodesics.

We shall use the Poincaré unit disc model of the hyperbolic plane. We shall use at the same time the Euclidean and the hyperbolic geometry of this disc.

With the notation of Figure 8, with s being the Euclidean distance from O to A in the Poincaré disc, and t being the Euclidean distance from the center O to the point M , we can write d and h as functions of s and t :

$$d(s) = \log \frac{1+s}{1-s} \quad \text{and} \quad h(t) = \log \frac{1+t}{1-t}.$$

Proposition 4.1. *Using the above notation, we have the following formulae for the quadrilaterals $OABC$ and $BCMA$ in terms of the Euclidean distance parameters s and t (Figure 10):*

$$\tanh L = \frac{\cos \alpha}{\sin \alpha} \frac{1-s^2}{2s} \quad \text{and} \quad t = \frac{\cos \alpha}{\sin \alpha + 1} s$$

Proof. We have the following relations:

$$\cosh d = \frac{1+s^2}{1-s^2} \quad \text{and} \quad \sinh d = \frac{2s}{1-s^2}$$

and

$$\cosh h = \frac{1+t^2}{1-t^2} \quad \text{and} \quad \sinh h = \frac{2t}{1-t^2}.$$

Equation (11) can be written as

$$\frac{\cosh(L+h)}{\cosh L} = \frac{1}{\sinh \alpha}$$

By applying the angle-addition formula, the equality becomes

$$\cosh h + \tanh L \sinh h = \frac{1}{\sin \alpha}.$$

On the other hand, Equation (9) shows that

$$\sinh d = \frac{1}{\tan \alpha \tanh L}$$

which in turn says

$$\tanh L = \frac{\cos \alpha}{\sin \alpha} \frac{1-s^2}{2s}.$$

By combining these equations, we have the following relation satisfied by the two Euclidean parameters s and t :

$$(19) \quad \frac{1+t^2}{1-t^2} + \frac{\cos \alpha}{\sin \alpha} \frac{1-s^2}{2s} \frac{2t}{1-t^2} = \frac{1}{\sin \alpha}$$

Factorizing in Equation (19), we get

$$(20) \quad \left(\frac{1+\sin \alpha}{\cos \alpha} t - s \right) \left(\frac{1+\sin \alpha}{\cos \alpha} ts + 1 \right) = 0$$

which in turn implies

$$(21) \quad t = \frac{\cos \alpha}{1+\sin \alpha} s.$$

We are using the fact that the second factor in 20 is always > 0 , since $t > 0$, and $s \cos \alpha > 0$. \square

Formula (21), which states that for α constant, the two parameters t and s are linearly related, has the following geometric interpretation. Consider the arc of hypercycle which is the set of points at hyperbolic distance L from the side BC . This arc starts at the vertex A and meets the side OC at a point, which we call M , which is hyperbolic distance h from O . The geometry of the Poincaré disc implies that the arc is a Euclidean circular arc, and we call the region surrounded by the line segment OA , the arc AM and the side MO , the central region of the quadrilateral. Note when $\alpha \geq \pi/2$, then $s \leq 0$, indicating that the central region appears on the other side of OA compared to the case $\alpha < \pi/2$.

As the moduli of convex quadrilaterals with three right angles has two parameters α and d , for a fixed angle α , we have a one-parameter family of right-angled quadrilaterals, with isometry type determined by d , or alternatively, by s .

The linear relation (21) between the values t and s says the following:

Proposition 4.2. *For a fixed angle α , as the value of d varies, the central region of the quadrilateral changes its shape via Euclidean homotheties, centered at the origin O , where the scaling is given by the value $s > 0$ with $d = \log \frac{1+s}{1-s}$.*

Now we come back to the hexagonal setting where three pentagons, or equivalently, six quadrilaterals, are combined. Type I hexagon is represented in Figure 11.

The hyperbolic lengths ℓ_i, L_i ($i = 1, 2, 3$) are all functions of d only, provided the angle moduli $(\alpha_1, \alpha_2, \alpha_3)$ are fixed.

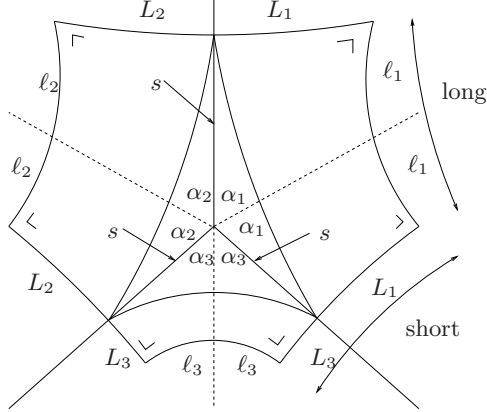


FIGURE 11. The central region has one s , which is the common Euclidean length of the three branches of the tripod T .

Equation (5) says that

$$\cosh \ell_i = \sin \alpha_i \cosh d.$$

By taking the ratio of the equality for i and j , we have

$$\frac{\cosh \ell_i}{\cosh \ell_j} = \frac{\sin \alpha_i}{\sin \alpha_j},$$

a quantity independent of d . Hence for different values of d and d' ,

$$\frac{\cosh \ell_i(d')}{\cosh \ell_j(d')} = \frac{\cosh \ell_i(d)}{\cosh \ell_j(d)}$$

for $1 \leq i, j \leq 3$.

This equality implies the following:

Proposition 4.3. *Suppose the angles $\alpha_1, \alpha_2, \alpha_3$ are fixed. As the value of d varies, the ratios among $\cosh \ell_1(d)$, $\cosh \ell_2(d)$ and $\cosh \ell_3(d)$ of the right-angled hexagons remain invariant.*

In other words, the ratios of weighted lengths (where taking the weighted length means replacing it by the hyperbolic cosine of that length) are invariant.

We concentrate on the deformations such that the long edges s_i get longer, or, equivalently, the scale of the central region gets larger. We can call these deformations *forward* deformations. The forward deformation of H makes *long edges longer and short edges shorter*. We recall that the angles α_i are constant for the forward deformations. In the limit of such a deformation, as $L_i \rightarrow 0$, one obtains ideal triangles.

Let us note by the way that unlike the deformation studied in the present paper, the deformations studied by Thurston in the paper [10] and by Papadopoulos-Th  ret in the paper [9] shrink the horocyclic/hypercyclic foliations and dilate the geodesic foliations.

The convergence $L_i \rightarrow 0$ is studied using the formula

$$\tanh L = \frac{\cos \alpha}{\sin \alpha} \frac{1 - s^2}{2s}$$

regardless of the cases $\alpha < \pi/2$ or $\alpha \geq \pi/2$. Note that $L \rightarrow 0$ and $s \rightarrow 1$ are equivalent, and that $s \rightarrow 1$ means that the long edge is being pushed to the geometric boundary of the Poincar   disc. Hence the one-parameter family of forward deformations provides a canonical path for the right-angled hexagon asymptotically converging to an ideal triangle. Also, in terms of elongating the long side by a factor

K (here $K = K(d)$) we can see from an equality obtained from the trigonometric formulae (5) and (9), namely,

$$\tanh^2 L(K) = \frac{\cos^2 \alpha}{\cosh^2(K\ell) - \sin^2 \alpha},$$

that $L(K)$ approaches zero as $K \rightarrow \infty$ along the forward deformation.

Let us consider the special “symmetric” case where $\alpha = \pi/3$, as this is the case treated in detail in [9]. Then six copies of the trirectangular quadrilateral (up to orientation) placed together form a right-angled hexagon with \mathbb{Z}_3 -rotational symmetry, which has side lengths $2L$ and 2ℓ appearing alternately.

Inserting the values $\alpha = \pi/3$ and $\ell = 0$ in the formula (5), we obtain

$$\frac{1}{\sqrt{3}/2} = \frac{\cosh d}{1}.$$

Since $\cosh d = 2s/(1-s^2)$, we get $s = 2 - \sqrt{3}$. This value of s is obtained by letting ℓ approach zero, or equivalently by letting the right-angled hexagon converge to an ideal triangle via “backward” deformations. The value of t then is $(2 - \sqrt{3})^2$. When deformed in the forward direction, the hexagon also converges to the ideal triangle, this time with $t = 2 - \sqrt{3}$ and $s = (2 - \sqrt{3})^2$. Note that the forward deformation is defined for all $K \geq 1$, while in general the backward deformation is not.

5. A GEOMETRIC LEMMA

Let us recall a few elements from [9].

A map f between two metric spaces is said to be *contracting* if $\text{Lip}(f) < 1$, and *weakly contracting* if $\text{Lip}(f) \leq 1$.

If f is a self-map of class $C^{0,1}$ of a convex domain Ω of the hyperbolic plane, then one can compute the norm of its differential at each point x of Ω ,

$$\|(df)_x\| = \sup_{V \in T_x \Omega \setminus \{0\}} \frac{\|(df)_x(V)\|}{\|V\|}.$$

Setting

$$\|df\| = \sup_{x \in \Omega} \|(df)_x\|,$$

we have the following

Proposition 5.1. *The quantity $\|df\|$ provides an upper bound for the global Lipschitz constant. In other words, we have*

$$\text{Lip}(f) \leq \|df\|.$$

In what follows, we consider maps between hyperbolic surfaces. The following statement will be used later in relating two hyperbolic surfaces.

Lemma 5.2. *Suppose there exist two pairs of orthogonal foliations (F_1, G_1) and (F_2, G_2) which are preserved by f (that is, f sends any leaf of F_1 onto a leaf of F_2 and any leaf of G_1 onto a leaf of G_2). If f is K -Lipschitz along the leaves of F_1 and contracting along the leaves of G_1 , then f is K -Lipschitz (that is, $\text{Lip}(f) \leq K$). Furthermore, if the map f stretches the leaves of F_1 by a constant factor K and if there exists an open geodesic segment contained in a leaf of F_1 which is sent to a geodesic segment contained in a leaf of F_2 (with length expanded by K), K is the best Lipschitz constant for f .*

Proof. The proof follows from an argument in [9] (p. 65-66) which we reproduce here. Consider the coordinate system (α, β) defined by the orthogonal grid formed by the leaves of F_1 and G_1 , where α and β are suitably chosen so that the coordinate

vector fields $(\frac{\partial}{\partial\alpha}, \frac{\partial}{\partial\beta})$ are an orthonormal basis for each tangent plane, and are linearly sent to an orthogonal basis by the differential df .

If $f = (f_\alpha, f_\beta)$, then

$$df_{(\alpha,\beta)} = \frac{\partial f_\alpha}{\partial\alpha} d\alpha + \frac{\partial f_\beta}{\partial\beta} d\beta.$$

Let $V = V_\alpha \frac{\partial}{\partial\alpha} + V_\beta \frac{\partial}{\partial\beta}$ a vector field with $\|V\| = 1$. The norm of the differential $\|df\|$ is computed as follows. First, we have

$$\begin{aligned} \|df_{(\alpha,\beta)}(V)\|^2 &= \left\| \frac{\partial f_\alpha}{\partial\alpha} V_\alpha \frac{\partial}{\partial\alpha} + \frac{\partial f_\beta}{\partial\beta} V_\beta \frac{\partial}{\partial\beta} \right\|^2 \\ &= \left(\frac{\partial f_\alpha}{\partial\alpha} V_\alpha \right)^2 + \left(\frac{\partial f_\beta}{\partial\beta} V_\beta \right)^2. \end{aligned}$$

From this, it follows that

$$\|df_{(\alpha,\beta)}(V)\| \leq \max_{\Omega} \left\{ \left| \frac{\partial f_\alpha}{\partial\alpha} \right|, \left| \frac{\partial f_\beta}{\partial\beta} \right| \right\} \|V\|$$

which in turn gives

$$\|df\| \leq \max_{\Omega} \left\{ \left| \frac{\partial f_\alpha}{\partial\alpha} \right|, \left| \frac{\partial f_\beta}{\partial\beta} \right| \right\}.$$

Now since the map f is K -Lipschitz along the leaves of F_1 , we have $\left| \frac{\partial f_\alpha}{\partial\alpha} \right| \leq K$ at any point of Ω . On the other hand since the map f is contracting along the leaves of G_1 , we have $\left| \frac{\partial f_\beta}{\partial\beta} \right| < 1$ at any point of Ω . Thus we have $\text{Lip}(f) \leq \|df\| \leq K$. \square

6. DEFORMING RIGHT-ANGLED HEXAGONS

Given three non-negative numbers (ℓ_1, ℓ_2, ℓ_3) , let H be a right-angled hexagon in the hyperbolic plane with pairwise non-consecutive side lengths $(2\ell_1, 2\ell_2, 2\ell_3)$. Such a hexagon is uniquely determined up to isometry by these three sides. Let us now consider these sides to be the *long* edges of H . We denote the lengths of the diametrically facing three pairwise non-consecutive sides (the *short* edges) by $\lambda_1, \lambda_2, \lambda_3$. If some ℓ_i is equal to 0, we consider that the corresponding side is at infinity. For any $K > 1$, we denote by H_K the right-angled hexagon with long edges of lengths $(2\ell_1(K), 2\ell_2(K), 2\ell_3(K))$, with $\ell_i(K)$, for $i = 1, 2, 3$, determined by

$$K = \frac{\cosh \ell_i(K)}{\cosh \ell_i}.$$

For $i = 1, 2, 3$, we define

$$(22) \quad k_i = \frac{\ell_i(K)}{\ell_i}$$

and we set

$$k = \max_i \{k_i\}.$$

Note that k is determined by H and K . We also note that from its definition, k is an increasing function of K and that when K varies from 1 to ∞ , so does k .

In the rest of this section, we construct a k -Lipschitz map $f_k : H \rightarrow H_K$ which is Lipschitz extremal in its homotopy class in the sense that the Lipschitz constant of any other map between the two given right-angled hexagons sending each edge of H to the corresponding edge of H_K is at least equal to k . Making K (or, equivalently, k) vary from 1 to ∞ , we obtain a family of marked right-angled hexagons which is a geodesic for the Lipschitz metric on the Teichmüller space of right-angled hyperbolic hexagons – a natural analogue of the metric defined above in (3). By gluing hexagons along their sides, we obtain families of geodesics for the arc metric

for the Teichmüller space of surfaces with nonempty boundary (and with variable lengths of the boundary components). Gluing surfaces with boundary along their boundary components and assembling the maps between them, we obtain geodesics for the Thurston metric on the Teichmüller space of surfaces without boundary (possibly with punctures).

The maps f_k that we construct from H to H_K preserve the two pairs of orthogonal partial foliations (F, G) and (F^K, G^K) of H and H_K respectively that we constructed in §2.

The k -Lipschitz map $f_k : H \rightarrow H_K$ satisfies the following conditions:

- (1) f_k stretches each long edge ℓ_i of H by the factor $k_i > 1$.
- (2) f_k sends each leaf of F to a leaf of F^K affinely (with respect to the natural arc-length parametrization) and it sends each leaf of G to a leaf of G^K .
- (3) The central region is sent to the central region.

Using the coordinates we established on each foliated pentagon P_i (the foliated rectangle with part of the foliated central region), the map f_k is defined by sending the point on H represented by (u_i, v_i) for some i to the point in H_K represented by the same coordinates (u_i, v_i) . This map is clearly a homeomorphism between H and H_K . It sends the leaves of F and G on H to those on H_K , and the central region to the central region. We will show a few properties of the map f_k , concluding that this map is Lipschitz extremal between the pair of right-angled hexagons.

Theorem 6.1. *The map f_k is an extremal k -Lipschitz map from H to H_K for all $K > 1$.*

We first recall another result in hyperbolic geometry stated as a lemma:

Lemma 6.2. *A segment of the hypercycle $F(u_i)$ with $0 \leq u_i \leq 1$, which projects onto a geodesic segment of length $r > 0$ on the long edge s_i via the nearest point projection map $\pi_i : P_i \rightarrow s_i$, has hyperbolic length $r(u_i)$, which is given explicitly by*

$$r(u_i) = \cosh(u_i L_i) r.$$

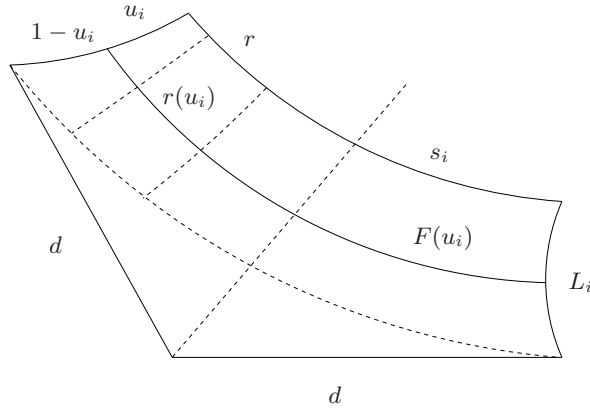


FIGURE 12.

Proof. We use the following elementary fact from the hyperbolic geometry of the upper-half plane model: The ray through the origin of slope $m = (\sinh u_i L)^{-1}$ is a set of points which are equidistant of $u_i L$ from the geodesic represented by the positive y -axis. (See Figure 12.) Then the hypercycle is represented by an oblique ray. The fibers of the nearest point projection map from the oblique ray to the positive y -axis are (subsets of) concentric circles centered at the origin. Hence in

order to prove the lemma it suffice to compute the hyperbolic stretching factor between the geodesic line segment between $(0, t_1)$ and $(0, t_2)$ with $t_2 > t_1$, and the hypercycle segment represented by the line segment between $(\frac{1}{\sqrt{1+m^2}}t_1, \frac{m}{\sqrt{1+m^2}}t_1)$ and $(\frac{1}{\sqrt{1+m^2}}t_2, \frac{m}{\sqrt{1+m^2}}t_2)$. We carry out this computation by comparing the hyperbolic norm of two paths $\sigma(t) = (0, t)$ and $\rho(t) = ((\frac{1}{\sqrt{1+m^2}}t, \frac{m}{\sqrt{1+m^2}}t)$ defined over $[t_1, t_2]$.

Recall that the length element in the upper-half plane is given by

$$ds^2 = \frac{dx^2 + dy^2}{y^2}.$$

Then the hyperbolic norms of the tangent vectors are given by

$$\|\sigma'(t)\| = \frac{1}{t}, \quad \|\rho'(t)\| = \frac{1}{t} \frac{\sqrt{1+m^2}}{m}.$$

By taking the ratio and replacing m by $(\sinh u_i L)^{-1}$, it follows that

$$\frac{\|\rho'(t)\|}{\|\sigma'(t)\|} = \frac{\sqrt{1+m^2}}{m} = \cosh u_i L,$$

a number independent of t . This proves that the nearest point projection induces a stretching between the geodesic and the hypercycle by the factor $\cosh u_i L$. \square

Proof of Theorem 6.1. Lemma 6.2 implies that each leaf $F_i(u_i)$ of the foliations F_i , for $0 \leq u_i \leq 1$, is obtained by stretching the geodesic segment $s_i = F_i(0)$ by the constant factor $\cosh(u_i L_i)$ and that each leaf $F_i^K(u_i)$ of the foliations F_i^K , for $0 \leq u_i \leq 1$, is obtained by stretching the geodesic segment $s_i^K = F_i^K(0)$ by the constant factor $\cosh(u_i L_i^K)$ where L_i^K is the length corresponding to L_i in the right-angled hexagon H_K . We note that $L_i^K < L_i$.

Since the map f_k sends the leaf $F_i(u_i)$ to $F_i^K(u_i)$, and the long edge s_i of length $2\ell_i$ to the long edge s_i^K of length $2k_i\ell_i$, the Lipschitz constant of f_k restricted to the leaf $F_i(u_i)$ is given by

$$\text{Lip}(f_k|_{F_i(u_i)}) = k_i \frac{\cosh(u_i L_i)}{\cosh(u_i L_i^K)} \leq k$$

where the inequality follows from $L_i^K < L_i$.

Concerning the foliation G_i , whose leaves are perpendicular to the leaves of F_i , for $0 \leq v_i \leq 2$, each leaf $G_i(v_i)$ of length L_i , namely the part of the leaf in the quadrilateral $P_i \setminus C$, is sent to the part of the leaf $G_i^K(v_i)$ in the quadrilateral $P_i^K \setminus C^K$ of length L_i^K . Thus the Lipschitz constant is

$$\text{Lip}(f_k|_{G_i(v_i)}) = \frac{L_i^K}{L_i} < 1 < k.$$

Our next task is to obtain a control on the Lipschitz constant of f_k in the central region of the hexagon. We divide the central region C into the three sectors $\{P_i \cap C\}_{i=1,2,3}$, whose interface is the geodesic tripod T centered at the origin O of the Poincaré disc, as discussed in §2.

Let $d(K)$ be the edge length of the tripod in the right-angled hexagon H_K , spanning the central region C_K . From the preceding discussion, we have $d(K) > d = d(1)$. We claim now that the map f_k restricted to each tripod edge has Lipschitz constant bounded above by k .

Since (by definition) the map f_k is an affine map on each edge, to show the Lipschitz constant bound, it suffices to obtain an estimate at one point. We do so at the point A_1 . Let Δs be an infinitesimal interval along the edge OA_1 at A_1 . By abuse of notation, we denote by Δs the hyperbolic length of that interval. Note that the edge OA_1 and the hypercycle $F_2(1, v_2)$ ($0 \leq v_2 \leq 2$) are tangent at A_1 .

Thus Δs corresponds to $\tilde{\Delta} s \subset s_2$ which is a multiple $\Delta s / \cosh L_1$ of Δs on s_2 . This follows from Lemma 6.2 via the nearest point projection $OA_1 \rightarrow s_2$ onto the long edge s_2 . The long edge s_2 is stretched by f_k by the factor k_2 , and the interval $\tilde{\Delta} s$ is mapped to $\hat{\Delta} s \subset s_2^K$. Thus the length element Δs on OA_1 now corresponds to $\hat{\Delta} s = k_2 \Delta s / \cosh L_1$ on s_2^K . Finally, via the canonical correspondence between the long edge s_2^K and the hypercycle $F_2^K(1, v_2)$ ($0 \leq v_2 \leq 2$) along the fibers of the nearest point projection $OA_1^K \rightarrow s_2^K$, Δs corresponds to an infinitesimal interval $\overline{\Delta} s \subset F_2^K(1, v_2)$ a multiple of Δs :

$$\frac{1}{\cosh L_1} k_2 \cosh L_1^K \Delta s.$$

The hypercycle $F_2^K(1, v_2)$ ($0 \leq v_2 \leq 2$) and the tripod edge OA_1^K are again tangent at A_1^K . Using the fact that $L_1^K < L_1$, we conclude that the Lipschitz constant of f_k restricted to the edge OA_1 at A_1 is equal to

$$\frac{\overline{\Delta} s}{\Delta s} = \frac{\cosh L_1^K}{\cosh L_1} k < k.$$

Therefore, we conclude that the Lipschitz constant of f_k restricted to the edge OA_1 is strictly less than k .

The region $P_i \cap C$ is foliated by the hypercycles equidistant from the long edge s_i , which are the leaves of $F_i(u_i)$ for $1 \leq u_i \leq 2$, whose endpoints are on the two edges $\overline{OA_j}$ and $\overline{OA_k}$ ($j, k \neq i$) of the tripod bounding the pentagon P_i . Hence $P_i \cap C$ is bounded by the two edges and the boundary hypercycle $F_i(1)$ of the central region $P_i \cap C$ equidistant from the long edge s_i by L_i .

We define a new function of u_i ,

$$\tilde{u}_i(u_i) = \frac{\text{the hyperbolic distance between } F_i(1) \text{ and } F_i(u_i)}{\text{the hyperbolic distance between } F_i(1) \text{ and the vertex } O}$$

for $1 \leq u_i \leq 2$. Note that $\tilde{u}_i(1) = 0$ and $\tilde{u}_i(2) = 1$. We also define $\tilde{u}_i^K(u_i)$ to be the corresponding function for the forward-deformed hexagon H_K , which is distinct from $\tilde{u}_i(u_i)$.

We claim that

$$\text{Lip}(f_k|_{F_i(u_i)}) = k_i \frac{\cosh(\tilde{u}_i L_i)}{\cosh(\tilde{u}_i^K L_i^K)} < k.$$

This follows from the facts that $L_i^K < L_i$ and that $\tilde{u}_i^K(u_i) < \tilde{u}_i(u_i)$ for $1 \leq u_i \leq 2$. The first inequality follows from the properties of the forward deformation f_K already seen. For the second inequality, note that the hypercycles $\{F_i^K(u_i)\}$ are more tightly packed in $P_i^K \cap C_K$ near the hypercycle $F_i^K(1)$ than the hypercycles $\{F_i^K(u_i)\}$ in $P_i \cap C$ near $F_i(K)$, which in turn implies $\tilde{u}_i^K(u_i) < \tilde{u}_i(u_i)$.

Now we study the Lipschitz constant of f_k restricted to the leaves of G_i in the central region $P_i \cap C$. We recall that the leaves $F_i(u_i)$ are parameterized proportionally to the arc length of the pair of the tripod edges $\overline{OA_j}$ and $\overline{OA_k}$ ($j, k \neq i$) of equal length d , as u_i varies in $[1, 2]$.

Let $\delta_i(u_i, v_i)$ be the hyperbolic distance between the point $G_i(v_i) \cap F_i(u_i)$ and the long edge s_i . First note that the function $\delta_i(u_i, v_i)$ is constant in v_i where it is defined. As v_i varies over $[0, 2]$, the range of δ_i varies, and it takes its maximal value for $v_i = 1$ when the endpoint of the leaf $G_i(1)$ is at the center O .

We define a function $w_i(u_i)$ in $u_i \in [1, 2]$ by restricting the function δ_i to the tripod edge $\overline{OA_j}$ (or equivalently to $\overline{OA_k}$) and subtracting the constant L_i from it. Namely, the value of $w_i(u_i)$ is the distance between the point (u_i, v_i) on $\overline{OA_j}$ (or equivalently to $\overline{OA_k}$) and the boundary hypercycle of the central region $P_i \cap C$. By observing how the leaves $F_i(u_i)$ intersect with the tripod edge $\overline{OA_j}$ modeled on the Poincaré disc, with the center O of H identified with the origin, we see that

the term $\frac{dw_i}{du_i}$ is equal to $d \cos \theta_i(u_i)$ where θ_i is the angle between the edge OA_j and the leaf $G_i(v_i)$. Note that $\theta(1) = \pi/2$ and $\theta_i(u_i)$ monotonically decreases as u_i increases, and goes down to the value $\alpha_i = \theta_i(2) < \pi/2$.

It then follows that the derivative of w_i in u_i is monotonically increasing and that

$$\lim_{u_i \rightarrow 1} \frac{dw_i}{du_i} = 0 \text{ and } \lim_{u_i \rightarrow 2} \frac{dw_i}{du_i} = d \cos \alpha_i.$$

The latter limit occurs at the vertex O . In other words, the function w_i is convex in u_i .

Defining the function w_i^K for H_K analogously, we have similarly:

$$\lim_{u_i \rightarrow 1} \frac{dw_i^K}{du_i} = 0 \text{ and } \lim_{u_i \rightarrow 2} \frac{dw_i^K}{du_i} = d(K) \cos \alpha_i.$$

We now claim that the function

$$R_i(u_i) = \left(\frac{dw_i^K}{du_i} \right) / \left(\frac{dw_i}{du_i} \right)$$

is increasing in $u_i \in [1, 2]$ and bounded above by:

$$\lim_{u_i \rightarrow 2} \left(\frac{dw_i^K(u_i)}{du_i} \right) / \left(\frac{dw_i(u_i)}{du_i} \right) = \frac{d(K)}{d} < k.$$

Namely, the claim says that the biggest stretch by f_K along the leaves of G_i occurs at the center of the hexagon on the leaf $G_i(1)$. The upper bound $d(K)/d$ is obtained from the ratio between the separation distances of leaves for F^K and F near the center of the hexagon, identified with the origin of the Poincaré disc.

This follows from the observation that for a given value of $u_i \in (1, 2)$, we have $\theta_i^K(u_i) > \theta_i(u_i)$, which follows from the comparison of the behavior of the Poincaré metric of the disc between the two Euclidean-homothetic regions C and C_K . Geometrically, when looking at the distributions of the leaves of $F_i(u_i)$ and $F_i^K(u_i)$ on C and on C_K , which are mutually Euclidean-homothetic in the Poincaré disc, the leaves for F_i^K are more tightly packed than the leaves of F_i near $u_i = 1$ (Figure 13). Hence for a particular pair of leaves $F_i(u_i)$ and $F_i^K(u_i) = f_K[F_i(u_i)]$, we have

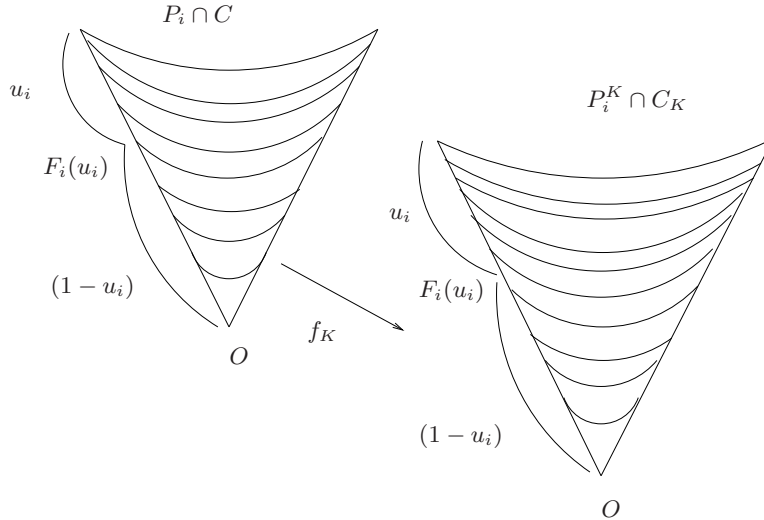


FIGURE 13. The foliations in the central region of the hexagon.

the inequality $\theta_i^K(u_i) > \theta_i(u_i)$. This comparison in turn shows that as a convex

function of u_i , $w_i(u_i)$ is more convex than the convex function $\frac{d}{d(K)}w_i^K(u_i)$. This implies the claim about $R_i(u_i) \leq \frac{d(K)}{d}$.

This in turn says that the rate of change

$$\frac{dw_i^K}{dw_i} = \left(\frac{dw_i^K}{du_i} \right) / \left(\frac{dw_i}{du_i} \right)$$

is bounded above by k_i , that is, since the map f_k send $P_i \cap C$ onto $P_i^K \cap C^K$, the stretching factor of the leaves of G_i is strictly less than k_i .

Combining these results, we conclude that for $1 \leq u_i \leq 2$,

$$\text{Lip}(f_k|_{G_i(v_i)}) < \frac{d(K)}{d} < k_i.$$

Now the map f_k sends the central region C to C_K and each open set P_i to P_i^K with norm $\|df_K\|$ of the differential bounded by k and it sends the tripod T to the tripod T_K with constant stretch ratio of $d(K)/d < k$. These three regions P_i can be glued along the tripod T , and the stretching Lipschitz constant remains less than k , proving that $f_k : H \rightarrow H_K$ is k -Lipschitz. \square

7. IDEAL TRIANGULATION OF A SURFACE AND THE CANONICAL DEFORMATIONS

So far we have considered a single right-angled hexagon, and its forward deformations. We consider now a hyperbolic surface S with boundary which is partitioned by a maximal sub-system of disjoint geodesic arcs into right-angled hexagons. Such a partition is usually called an ideal triangulation T on S (see e.g. [7].) We denote this combinatorial data by (S, T) . The gluing edges of the hexagons whose union constitutes the surface S are considered as the long edges, and the edges appearing as part of the boundary components of S are considered as the short edges.

We use the notation of §2. By stretching each long edge s_i of a hexagon by a factor $k_i > 1$ satisfying Equation (22), the canonical deformations between hexagons define a map, which we still denote $f_k : S \rightarrow S_K$, from the hyperbolic surface with boundary S to the hyperbolic surface with boundary S_K obtained by gluing the image hexagons. Here, k is the maximum among the stretching factors k_i , with i indexing the long edges of all the right-angled hexagons. This map f_k makes each boundary component shorter.

Proposition 7.1. *The Lipschitz map $f_k : S \rightarrow S_K$ is an extremal k -Lipschitz map. That is, this map is a k -Lipschitz homeomorphism, and for any $k' < k$, there is no k' -Lipschitz homeomorphism from S to S_K in the same homotopy class preserving the boundary.*

Proof. We use Lemma 5.2 and we note that when two hexagons H^α and H^β are glued along a long edge e , the foliations F^α, G^α and F^β, G^β are glued together to form a new orthogonal pair of foliations on the union of the image hexagons. The constructed maps between the hexagons satisfy the properties required by the proposition, and the hexagons glue together as well. \square

The following theorems are proved in the same way as Theorem 7.3 of [9]; we do not repeat the arguments here. In the following statements, we take the point of view where each map $f_k : S \rightarrow S_K$ is an element, which we also denote by (S, f_k) , of the Teichmüller space of S , that is, a marked hyperbolic structure.

Theorem 7.2. *By letting K vary from 1 to ∞ , we get a family of maps $f_k : S = S_1 \rightarrow S_K$ which, as a path in Teichmüller space, is a geodesic for the arc metric and for the Lipschitz metric on $\mathcal{T}(S)$.*

Theorem 7.3. *The Lipschitz and the arc metrics on $\mathcal{T}(S)$ coincide on the path (S, f_k) , $k \geq 1$. More precisely, we have, for any $K_1 \leq K_2$,*

$$d([(S, f_{K_1})], [(S, f_{K_2})]) = L([(S, f_{K_1})], [(S, f_{K_2})])$$

where d and L are the arc and Lipchitz metrics respectively.

By gluing surfaces with boundary along the totally geodesic boundary components, we also get geodesics for the Lipschitz metric for surfaces without boundary, as in [9].

As mentioned in the introduction, the resulting geodesics for a surface S with boundary are distinct from the geodesics constructed by Thurston using the stretch line construction where the ideal triangles spiral along the boundary components of S . For surfaces with more than one boundary component, this follows from the fact that Thurston's path causes the lengths of all boundary components change by the same factor, whereas our deformation causes the length of each boundary components to change at different factors in general.

There is a relation between our coordinates on right-angled hexagons and coordinates constructed by Luo in [7] for the Teichmüller space of a surface with boundary. Luo calls his coordinate functions *radius coordinates*. In our context, they correspond to the sum of the lengths L_i . To be more precise, consider two right-angled hexagons H^α and H^β , sharing a long edge of the same length, which we call the edge $e_{\alpha\beta}$. The edge $e_{\alpha\beta}$ borders two strips, each foliated by leaves equidistant from the edge $e_{\alpha\beta}$ bordered on the other end by the sides of the central regions in H^α and H^β . In our notation, the widths of the strips, namely the distances from the shared edge to the respective central regions, are called $L^\alpha(e_{\alpha\beta})$ and $L^\beta(e_{\alpha\beta})$. The radius coordinate of Luo is equal to

$$z(e_{\alpha\beta}) = \frac{L^\alpha(e_{\alpha\beta}) + L^\beta(e_{\alpha\beta})}{2}.$$

By setting E to be the set of long edges of an ideal triangulation T with respect to a hyperbolic metric on a surface S with totally geodesic boundary, we can consider the set of functionals $z : E \rightarrow \mathbb{R}$ on the space of hyperbolic metrics of the surface with totally geodesic boundary. Luo calls $z(e)$ the radius invariant of e , and z the radius coordinate system of (S, T) .

In [7], the following is shown:

Theorem 7.4. *Given an ideal triangulation (S, T) on a compact surface S with boundary, each hyperbolic metric with totally geodesic boundary on S is determined up to isotopy by its radius coordinates. Furthermore, the image of the map z is a convex polytope satisfying the following two properties: for each fundamental edge cycle e_1, \dots, e_k*

$$\sum_{j=1}^k z(e_j) > 0$$

and for each boundary edge cycle e_1, \dots, e_n corresponding to the boundary component of length ℓ ,

$$\sum_{i=1}^n z(e_i) = \ell.$$

Finally, we mention that D. Alessandrini and V. Disarlo informed us that they have work in progress in which they define “generalized stretch lines” for surfaces with boundary and they prove that every two hyperbolic structures can be joined by a geodesic segment which is a finite concatenation of such generalized stretch lines, cf. [3].

Acknowledgements The authors are grateful to the referee for his thorough reading and his valuable corrections.

REFERENCES

- [1] N. A'Campo and A. Papadopoulos, Notes on non-Euclidean geometry, in *Strasbourg Master Class on Geometry* (A. Papadopoulos, ed.) IRMA Lectures in Mathematics and Theoretical Physics Vol. 18, European Mathematical Society, Zurich, 2012, p. 1-182.
- [2] D. Alessandrini, L. Liu, A. Papadopoulos and W. Su, The horofunction compactification of the arc metric on Teichmüller space. *Topology Appl.* 208 (2016), 160–191.
- [3] D. Alessandrini and V. Disarlo, Generalized stretch lines for surfaces with boundary, in preparation.
- [4] W. Fenchel, Elementary geometry in hyperbolic space. De Gruyter Studies in Mathematics, 11. Berlin, Walter de Gruyter & Co., 1989.
- [5] L. Liu, A. Papadopoulos, W. Su and G. Théret, On length spectrum metrics and weak metrics on Teichmüller spaces of surfaces with boundary. *Ann. Acad. Sci. Fenn., Math.* 35, No. 1, 255–274 (2010).
- [6] L. Liu, A. Papadopoulos, W. Su and G. Théret, Length spectra and the Teichmüller metric for surfaces with boundary, *Monats. Math.*, vol. 161, no3, pp. 295-311 (2010).
- [7] F. Luo, On Teichmüller spaces of surfaces with boundary, *Duke Math. J.* 139 (2007) 463–481.
- [8] A. Papadopoulos and G. Théret, Shortening all the simple closed geodesics on surfaces with boundary, *Proc. Am. Math. Soc.* 138 (2010), No. 5, p. 1775-1784.
- [9] A. Papadopoulos and G. Théret, Some Lipschitz maps between hyperbolic surfaces with applications to Teichmüller theory, *Geom. Ded.* 161 (2012), 63-83.
- [10] W. P. Thurston, Minimal stretch maps between hyperbolic surfaces. 1986 preprint, arxiv:math/9801039v1.

ATHANASE PAPADOPOULOS, UNIVERSITÉ DE STRASBOURG AND CNRS, 7 RUE RENÉ DESCARTES, 67084 STRASBOURG CEDEX, FRANCE

E-mail address: `athanase.papadopoulos@math.unistra.fr`

SUMIO YAMADA, GAKUSHUIN UNIVERSITY, 1-5-1 MEJIRO, TOKYO, 171-8588, JAPAN

E-mail address: `yamada@math.gakushuin.ac.jp`